



Dynamic analysis of N-glycomic and transcriptomic changes in the development of ovarian cancer cell line A2780 to its three cisplatin-resistant variants

Guiling Lin^{1#}, Ran Zhao^{1#}, Yisheng Wang¹, Jing Han², Yong Gu², Yiqing Pan², Changhao Ren², Shifang Ren², Congjian Xu^{1,3,4,5}

¹Department of Gynecology, Obstetrics and Gynecology Hospital of Fudan University, Shanghai 200011, China; ²NHC Key Laboratory of Glycoconjugates Research, Department of Biochemistry and Molecular Biology, School of Basic Medical Sciences, Fudan University, Shanghai 200032, China; ³Department of Obstetrics and Gynecology of Shanghai Medical School, Fudan University, Shanghai 200032, China; ⁴Shanghai Key Laboratory of Female Reproductive Endocrine Related Diseases, Shanghai 200032, China; ⁵Institute of Biomedical Sciences, Fudan University, Shanghai 200032, China

Contributions: (I) Conception and design: C Xu, S Ren; (II) Administrative support: None; (III) Provision of study materials or patients: G Lin, R Zhao; (IV) Collection and assembly of data: G Lin, R Zhao; (V) Data analysis and interpretation: All authors; (VI) Manuscript writing: All authors; (VII) Final approval of manuscript: All authors.

[#]These authors contributed equally to this work.

Correspondence to: Congjian Xu, PhD. Department of Gynecology, Obstetrics and Gynecology Hospital of Fudan University, 419 Fang-Xie Road, Shanghai 200011, China. Email: xucongjian@fudan.edu.cn; Shifang Ren, PhD. NHC Key Laboratory of Glycoconjugates Research, Department of Biochemistry and Molecular Biology, School of Basic Medical Sciences, Fudan University, 138 Yi-Xueyuan Road, Shanghai 200032, China. Email: renshifang@fudan.edu.cn.

Background: Platinum resistance development is a dynamic process that occurs during continuous chemotherapy and contributes to high mortality in ovarian cancer. Abnormal glycosylation has been reported in platinum resistance. Many studies on platinum resistance have been performed, but few of them have investigated platinum resistance-associated glycans based on N-glycomics. Moreover, glycomic alterations during platinum resistance development in ovarian cancer are rarely reported. Therefore, the objective of this study was to determine platinum resistance-related N-glycans in ovarian cancer cells during continuous exposure to cisplatin. These glycans might be involved in the mechanism of platinum resistance and serve as biomarkers to monitor its development.

Methods: This study mimicked the development of platinum resistance in ovarian cancer by continuously exposing A2780 cells to cisplatin. Cisplatin-resistant variants were confirmed by higher half maximal inhibitory concentration (IC₅₀) values and increased P-glycoprotein (ABCB1, P-gp) expression compared to A2780 cells. Analysis of dynamic N-glycomic changes during the development of platinum resistance in cisplatin-resistant variants was performed with MALDI-time-of-flight (TOF)-MS combined with ethyl esterification derivatization, which were used to discriminate between α 2,3- and α 2,6-linkage N-acetylneuraminic acid. N-glycan alterations were further validated on a glycotransferase level via transcriptome sequencing and real-time PCR (RT-PCR).

Results: Compared to the A2780 cells, MS analysis indicated that α 2,3-linked sialic structures and N-glycan gal-ratios were significantly higher, while fucosylated glycans were lower in three cisplatin-resistant variants. Transcriptome sequencing and RT-PCR showed that gene expression of *ST3GAL6* and *MGAT4A* increased, while gene expression of *FUT11*, *FUT1*, *GMDS*, and *B4GALT5* decreased in three cisplatin-resistant variants.

Conclusions: Analysis of N-glycans and glycone expression showed that α 2,3-linked sialic structures might serve as biomarkers to monitor the development of platinum resistance and to guide individualized treatment of ovarian cancer patients.

Keywords: Ovarian cancer; platinum resistance; glycomic; glycogene expression analysis

Submitted Dec 17, 2019. Accepted for publication Jan 30, 2020.

doi: 10.21037/atm.2020.03.12

View this article at: <http://dx.doi.org/10.21037/atm.2020.03.12>

Introduction

Ovarian cancer is the seventh most common cancer in women around the world and its mortality rate is second among gynecological cancers (1). Platinum and paclitaxel combination chemotherapy is a first-line postoperative regimen for ovarian cancer patients. Although 80% of patients have an initial response to platinum compounds, up to 70% of ovarian cancer patients will relapse and become resistant to platinum in the process of chemotherapy (2). Platinum resistance development is a dynamic process that occurs during continuous cycles of chemotherapy. Therefore, studies on the dynamic process involved in the development of platinum resistance should be performed during chemotherapy. This may provide a better understanding of platinum resistance, identify biomarkers needed to monitor platinum resistance, guide ovarian cancer patient treatment, and improve patient 5-year survival. For those ovarian cancer patients resistant to chemotherapy, monitoring is vital for avoiding delays in the effective treatment and unnecessary chemotherapy side effects (3). Thus, it is urgent to develop useful biomarkers for monitoring platinum resistance and to study the development of platinum resistance (4).

Glycosylation is one of the most common posttranslational modifications and is responsible for modulating and controlling the biological roles of glycoproteins and plays an important role in many physiological and pathological processes (5-8). Abnormal glycosylation related to drug resistance has been reported in several research studies (9-11). First, the sensitivity to platinum was altered in ovarian cancer after glycosylation of drug transporters was inhibited, such as P-glycoprotein, breast cancer resistance protein (BCRP, ABCG2), multidrug resistance protein 1 (MRP1, ABCC1), and multidrug resistance protein 4 (MRP4, ABCC4) (12,13). Second, aberrant glycosylation in some signaling pathways is also involved in the mechanisms of drug resistance. For instance, the phosphoinositide 3 kinase (PI3K)/Akt pathway was aberrantly activated by the glycosylation modification result in multidrug resistance (14,15). Third, few serum samples, provided by late-stage recurrent ovarian cancer patients

before and after receiving an experimental drug treatment (i.e., a combination of docetaxel and imatinib mesylate), were analyzed to identify specific changes in protein glycosylation related to cancer progression. The results indicated that altered glycosylation of serum glycoprotein may be a potential biomarker for progression of ovarian cancer (16). Therefore, glycans are important predictive biomarkers and are crucial for the mechanism of drug resistance.

To the best of our knowledge, few glycomic analyses were performed on drug-resistant ovarian cancer and none of them focused on the dynamic process of chemotherapy (17). Due to heterogeneity and accessibility limitations of the clinical samples, a cancer cell line was chosen as an experimental model to study N-glycan alterations during continuous exposure to cisplatin. Moreover, cancer cells are more stable than clinical samples and are more convenient for mechanistic research (18). The present study mimics the development of platinum resistance development in ovarian cancer by continuously exposing A2780 cells to cisplatin. Cisplatin-resistant variants were established after 20, 30, and 40 continuous exposures to cisplatin and were confirmed by higher half maximal inhibitory concentration (IC_{50}) values and increased ABCB1 expression compared to A2780 cells. Analysis of N-glycomic dynamic changes during the development of platinum resistance in cisplatin-resistant variants was performed using MALDI-time-of-flight (TOF)-MS. N-glycan alterations associated with platinum resistance were further validated on a glycotransferase level using transcriptome sequencing and real-time PCR (RT-PCR). To date, this is the first attempt to discover specific N-glycan changes in ovarian cancer cells during continuous exposure to cisplatin, which may provide more information about glycan biomarkers of platinum resistance and related cisplatin resistance mechanisms.

Methods

Cell culture and reagents

An ovarian cancer cell line A2780 and three cisplatin-resistant variants were cultured in Roswell Park Memorial

Institute (RPMI)-1640 medium (BasalMedia Technologies, Shanghai, China) supplemented with 10% fetal bovine serum (Moregate Biotech, Melbourne, Australia) and 1% penicillin/streptomycin (Invitrogen, Carlsbad, USA) at 37 °C in a humidified atmosphere of 5% CO₂. Three cisplatin-resistant variants of A2780 cells were regularly stimulated with 3 µg/mL cisplatin (Abcam, Cambridge, UK) and subcultured once in drug-free medium before the experiment.

In this study, Milli-Q water (MQ) was generated from a Q-Gard 2 system (Millipore, Amsterdam, Netherlands). Sodium dodecyl sulfate (SDS), phosphate buffered saline (PBS), ethanol, and trifluoroacetic acid (TFA) were purchased from Merck (Merck, Darmstadt, Germany). Sodium hydroxide (NaOH), urea, dithiothreitol, ammonium bicarbonate, iodoacetamide, 1-ethyl-3-(3-dimethylaminopropyl)-carbodiimide (EDC) hydrochloride, and 1-hydroxybenzotriazole (HOBt) hydrate were obtained from Sigma-Aldrich (Sigma-Aldrich, St. Louis, MO, USA). Recombinant peptide-N-glycosidase F (PNGase F), Nonidet P-40 (NP-40), and denaturation buffer were bought from Roche Diagnostics (Roche Diagnostics, Mannheim, Germany). Acetonitrile (ACN) and 2,5-dihydroxybenzoic acid (2,5-DHB) were from Bruker Daltonics (Bruker Daltonics, Bremen, Germany) and Biosolve (Biosolve, Valkenswaard, Netherlands), respectively.

Cell selection strategy

A2780 cells were plated in duplicate into six-well plates at a density of 5×10^5 cells per well and a control plate was set up separately. Once the cell culture reached 70% confluency, 2 mL of media with 3 µg/mL cisplatin were added to all plates excluding the control, which received 2 mL of drug-free medium. After incubation for 48 h at 37 °C with 5% CO₂, the drug was removed and replaced by fresh drug-free culture medium. Once the cell culture reached 90% confluency, cells from one control plate and one drug plate were removed and counted. Cells from both plates were re-plated in duplicate into a six-well plate at a density of 5×10^5 cells per well and cultured until reaching 70% confluency for the next cisplatin exposure. These steps were repeated until reaching a total number of 40 cycles. The fold resistance were calculated when the 20th, 30th, and 40th cycles were done, which showed significant differences compared to A2780 cells. The three cisplatin-resistant variants were stored at -80 °C and named A2780-R1,

A2780-R2, and A2780-R3, respectively. Cells were thawed together for cytotoxicity analysis and fold resistance calculations (19,20) (*Figure 1*).

CCK8 assay

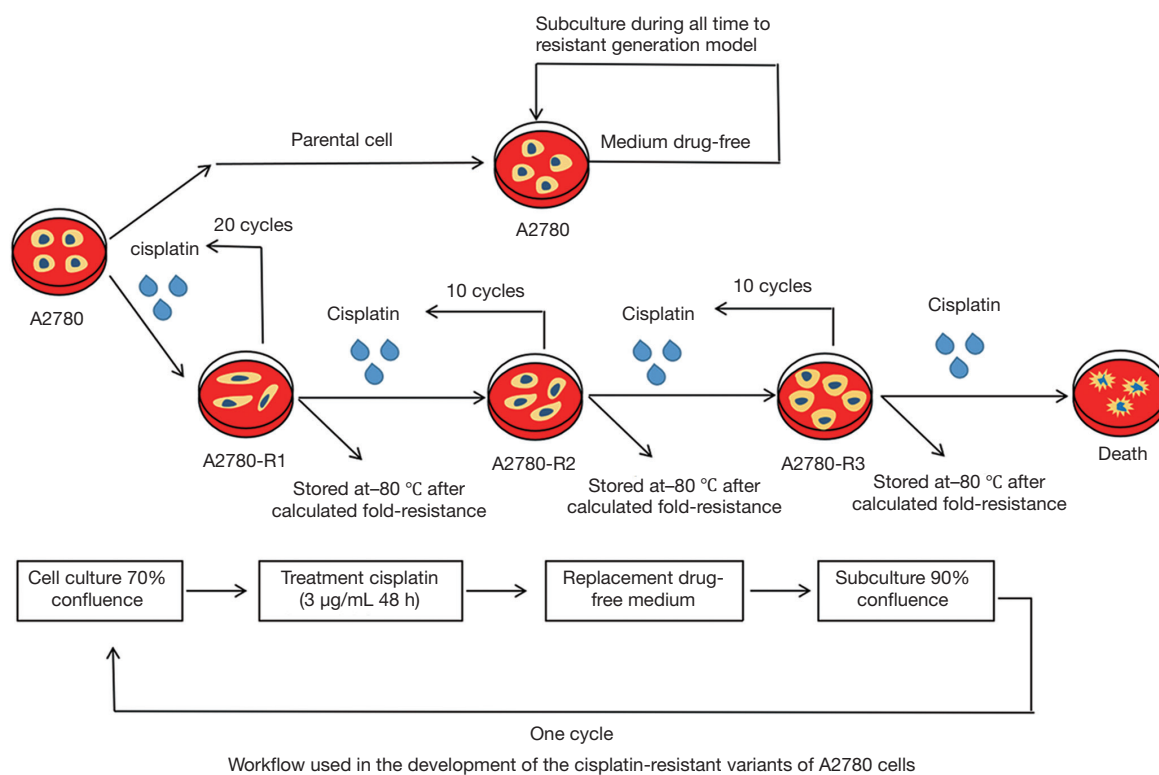
Cell growth and viability were measured using the CCK8 assay (Dojindo, Kumamoto, Japan). Briefly, A2780 cells and three cisplatin-resistant variants were seeded into 96-well plates (5,000 cells/well). After 12 h, cells were treated with various concentrations of cisplatin (0, 0.5, 1, 2, 4, 8, 16, 32, and 64 µg/mL) for 48 h. Then, 10 µL of the CCK8 reagent were added to the cells and absorbance at 450 nm was measured by an EPOCH ELISA reader (BioTek Instruments, Vermont, USA) according to the manufacturer's instructions.

Cell lysis preparation for mass spectrometry (MS) analysis

Cells were rinsed twice with PBS. After washing, 2% SDS-containing protease inhibitor cocktail (Roche Diagnostics, Roche Applied Science, Meylan, France) was used to lyse the cells on ice for 30 min. The lysate was then boiled for 15 min before centrifugation at 14,000 g for 30 min and the supernatant was collected for protein concentration quantification using a BCA kit (Thermo Scientific, San Jose, CA, USA).

Release and purification of N-glycans from glycoprotein

A total of 1 mg of protein from the supernatant was added to 200 µL of 2% SDS-containing 8-M urea and 10-mM dithiothreitol. The sample was heated to 56 °C for 20 min and then incubated in 40-mM ammonium bicarbonate containing 25-mM iodoacetamide at 37 °C for 30 min in the dark. Subsequently, the sample was transferred to an ultrafiltration unit (Amicon Ultra-0.5, Ultracel-10 membrane; Millipore, Billerica, MA, USA) and centrifuged at 14,000 g for 15 min. The sample was washed by adding 200 µL of 1× PBS to the ultrafiltration unit. Afterwards, 3–5 µL of PNGase F, 20 µL of NP-40, 20 µL of denaturation buffer, and 160 µL of 1× PBS were added to the device and incubated with 250 rpm shaking for 24 h at 37 °C. The ultrafiltration unit was transferred to a new collection tube before centrifuging at 14,000 g for 15 min. The filter membrane was then washed with 200 µL of 1× PBS three times. N-glycans from the collection tube were purified and desalted using Porous Graphitic Carbon



Workflow used in the development of the cisplatin-resistant variants of A2780 cells

Figure 1 Workflow used for the development of cisplatin-resistant variants of A2780 cells. Steps were repeated for a total of 40 cycles. Three cisplatin-resistant variants were frozen after cycle 20, 30, and 40 (named A2780-R1, A2780-R2, and A2780-R3, respectively).

Solid-Phase Extraction (PGC-SPE). The PGC-SPE microcolumn, a GELoader tip filled with porous graphic carbon powder, was preconditioned with three volumes of 0.1% (v/v) TFA in 80% (ACN)/H₂O (v/v) and equilibrated with three volumes of 0.1% (v/v) TFA. The sample was passed through the microcolumn five times to achieve complete glycan adsorption. Subsequently, the microcolumn was washed with two volumes of water to remove salts and buffer. Finally, N-glycans were eluted with 200 µL of 25% (v/v) ACN containing 0.05% (v/v) TFA and lyophilized in a vacuum freeze dryer (Martin Christ GmbH, Osterode, Germany).

Derivatization and enrichment of N-glycans

Lyophilized glycans were added to 100 µL of 250-mM EDC and 250-mM HOBt in ethanol and incubated for 1 h at 37 °C. Then, 100 µL of ACN were added and the mixture was incubated at -20 °C for 15 min. Subsequently, the mixture was brought to room temperature before glycan purification using a cotton HILIC microtip. For purification of the derived N-glycans, 10-µL pipette tips

were packed with a 3-mm cotton thread. Cotton HILIC tips were pre-wetted three times with 10 µL of MQ water and then equilibrated with 10 µL of 85% ACN three times. Samples were loaded by carefully pipetting up and down 50 times. The tips were washed three times with 10 µL of 85% ACN/1% TFA, and three times with 10 µL of 85% ACN. In the end, N-glycans were eluted in 10 µL of MQ water by pipetting up and down 50 times (18,21).

MALDI-TOF-MS analysis

The TOFMix™ (LaserBio Laboratories, France) was used for calibration before MS analysis. A total of 5 µL of derivatized N-glycans were premixed with 5 µL of sDHB matrix (5 mg/mL in 50% ACN with 1-mM NaOH) and 2 µL of the mixture were spotted on a MALDI target plate (800/384 MTP AnchorChip, Bruker Daltonics, Bremen, Germany). Each sample was spotted in three replicates and spots were allowed to air dry at room temperature, followed by a MALDI-TOF-MS measurement. Profiles were generated by two laser shots and a total of 200 profiles were accumulated from different points of laser irradiation into

Table 1 Summary of primer sequences for RT-PCR analysis

Primer-name	Sequence (5' to 3')
ST3GAL6-forward	TGGCCTTAGTCTTGTGTCC
ST3GAL6-reverse	CTACTATGGAAACGCCACCA
MGAT4A-forward	AAAGAGCGTCTTCGAGTGGC
MGAT4A-reverse	ACTTCCATTAGTCTCTGCTCCA
B4GALT5-forward	ACGCACAACGCCTTCACTGG
B4GALT5-reverse	GGGAGAGAGCAGCGGGACAG
FUT11-forward	GCGGGTGGGAGGCTGAG
FUT11-reverse	ACACTGGTAGGTCCACGGTCTC
FUT1-forward	GCAGGCCATGGACTGGTT
FUT1-reverse	CCTGGGAGGTGTCGATGTTT
GMDS-forward	TTTAATACGGGTCAATTGAGCA
GMDS-reverse	TGAGATCGCCATAGTGCAACT
GAPDH-forward	TGACTTCAACAGCGACACCCA
GAPDH-reverse	CACCCTGTTGCTGTAGCCAAA

RT-PCR, real-time PCR.

one file for each sample spot.

MS data for N-glycans was pre-processed, normalized and extracted using the Progenesis MALDI software (Shimadzu Biotech, Kyoto, Japan). Relative intensity for each N-glycan was calculated by dividing the intensity of that N-glycan by the sum intensity of all identified N-glycans. Relative standard deviation (RSD) for relative intensity values was used to estimate the MS stability. In this study, RSD for the 77 N-glycans was <25%. The threshold of intensity ratios was set at 1.2 and 0.83 to estimate up- or down-regulation, respectively. Significant differences in N-glycans and glyco-subclasses were analyzed using Student's *t*-test and $P < 0.05$ was considered statistically significant. The proposed structures of identified glycans were interpreted manually based on their *m/z* values according to several published studies, GlycoWorkbench, and Glycan Mass Spectral Database.

Total RNA extraction and transcriptome sequencing

Total RNA was extracted using the TRIzol™ reagent (Invitrogen, Carlsbad, CA, USA). Transcriptome sequencing was conducted by OE Biotech Co., Ltd. (OE Biotech Co., Ltd, Shanghai, China). Glycogenes were searched and selected using the following keywords: “glyco”,

“glycan”, “gluc”, “gal”, “mgat”, “st6”, “st3”, “gnt”, “galnt”, “fuc”, “mannose”, and “alg”.

Quantitative RT-PCR (qRT-PCR) analysis

Total RNA was extracted with TRIzol-up (EZBioscience, China) and 2 µg of RNA were used for reverse transcription with the 4× Reverse Transcription Master Mix (EZBioscience, China). The 2× SYBR Green qPCR Master Mix (EZBioscience, China) was used to perform qRT-PCR. Subsequently, RT-PCR analysis was carried out using the ABI 7500 Fast Real-time PCR system (Applied Biosystems, Switzerland). According to the manufacturer's instructions, the cycling steps were as follows: reverse transcription (15 min, 42 °C), activation of the Hot-Star DNA Polymerase (5 min, 95 °C), and amplification for 40 cycles (10 s at 95 °C, 40 s at 60 °C). The mRNA level was calculated by $2^{-\Delta\Delta C_t}$ with GAPDH as an internal control. Primer sequences are shown in *Table 1*.

Western blot analysis

Total protein was extracted from cells with 2% SDS containing a protease inhibitor cocktail (Roche Diagnostics, Roche Applied Science, Meylan, France) on ice for 30 min. Lysates were boiled for 15 min before centrifugation at 14,000 g for 30 min, and the supernatant was collected for protein concentration quantification using a BCA kit (Thermo Scientific, San Jose, CA, USA). A total of 30 mg of proteins were separated using 10% SDS-PAGE gels by electrophoresis and transferred to PVDF membranes. After blocking with 5% skim milk, the membranes were incubated with a primary antibody at room temperature for 3 h and washed with TBST three times. The membranes were then incubated with HRP-conjugated polyclonal goat antibodies (secondary antibodies) at room temperature for 1 h and washed with TBST three times again. Finally, the protein bands were visualized with the Tannon™ High-sig ECL Western Blotting Substrate (Tannon, Shanghai, China). GAPDH (Cell Signaling Technology, Danvers, MA, USA) was used as an internal control. The p-gp antibodies (Cell Signaling Technology, Danvers, MA, USA) were diluted 1:1,000 in this study.

Statistical analyses

Results are represented as mean ± standard deviation (SD). Significant differences were analyzed using Student's *t*-test

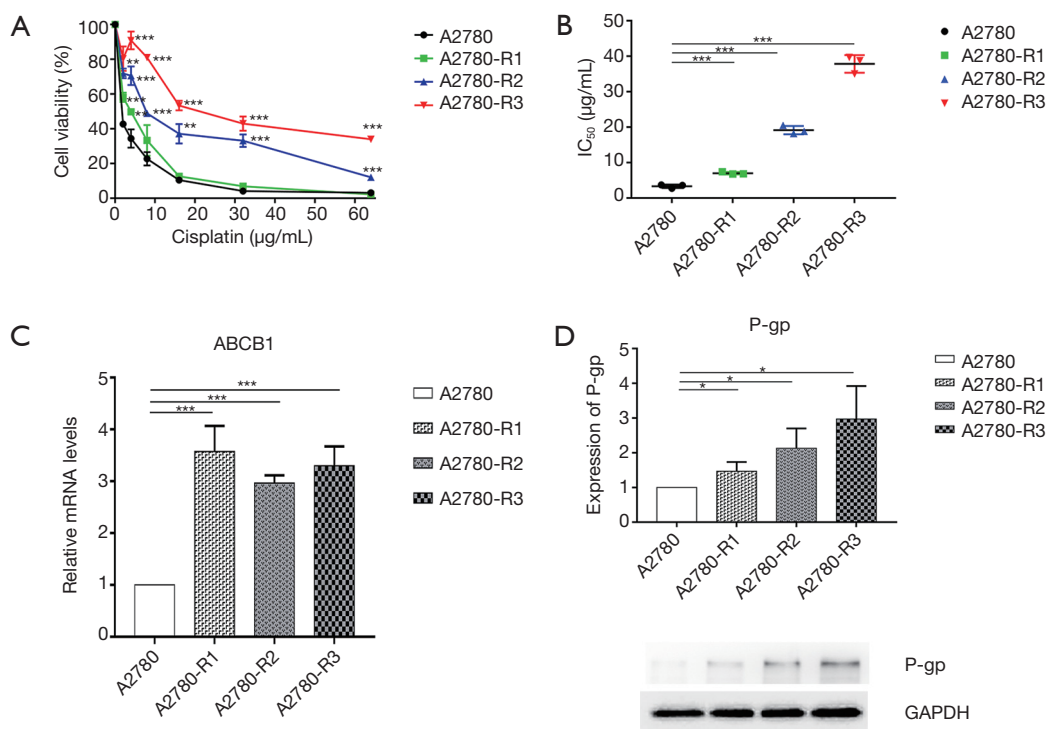


Figure 2 Viability of A2780 cells and three cisplatin-resistant variants after cisplatin incubation for 48 h was evaluated using CCK8 assay. (A) CCK8 analysis of A2780 cells and three cisplatin-resistant variants; (B) IC₅₀ of A2780 cells and three cisplatin-resistant variants; (C,D) expression of ABCB1 among A2780 cells and three cisplatin-resistant variants were determined by qPCR and Western blot. Error bars: SD (repeated three times); *, P<0.05; **, P<0.01; ***, P<0.001, differences were evaluated using Student's *t*-test. SD, standard deviation; IC₅₀, half maximal inhibitory concentration; qPCR, quantitative PCR.

and SPSS (version 16.0; SPSS Inc., Chicago, IL, USA) software, where P<0.05 was considered statistically significant. Results were visualized using GraphPad Prism (version 7).

Results

Cisplatin sensitivity and ABCB1 expression in A2780 cells and three cisplatin-resistant variants

Three cisplatin-resistant variants of the A2780 cells were established during continuous exposure to cisplatin. Fold resistance of three cisplatin-resistant variants was calculated when treated with cisplatin for the 20th, 30th, and 40th cycles, which showed significant differences compared to their parental A2780 cells. The three cisplatin-resistant variants were named A2780-R1, A2780-R2, and A2780-R3, respectively and stored at -80 °C together with A2780 cells. Then, cells were thawed for cytotoxicity analysis and fold resistance calculation was performed. The CCK8 assay

was used to evaluate drug resistance of the three cisplatin-resistant variants (Figure 2A). IC₅₀ of the parental A2780 cells was obtained at a concentration of 3.32±0.51 µg/mL, while IC₅₀ for three cisplatin-resistant variants was established at a concentration of 7.00±0.36, 19.15±1.17, and 37.83±2.47 µg/mL, respectively (Figure 2B). Meanwhile, ABCB1 expression in A2780 cells and three cisplatin resistance variants was determined via RT-PCR and Western blotting. The results are shown in Figure 2C,D. Increased expression of ABCB1 indicated the emergence of a resistant phenotype in three cisplatin-resistant variants.

Morphology and growth rate comparison among A2780 cells and three cisplatin resistance variants

The morphology and growth rates of A2780 cells and three cisplatin-resistant variants were compared by taking photos and counting cells after plating into six-well plates at the same cell density for 48 h (Figure 3A,B,C,D). Compared to parental A2780 cells, A2780-R1 cells appeared flattened and

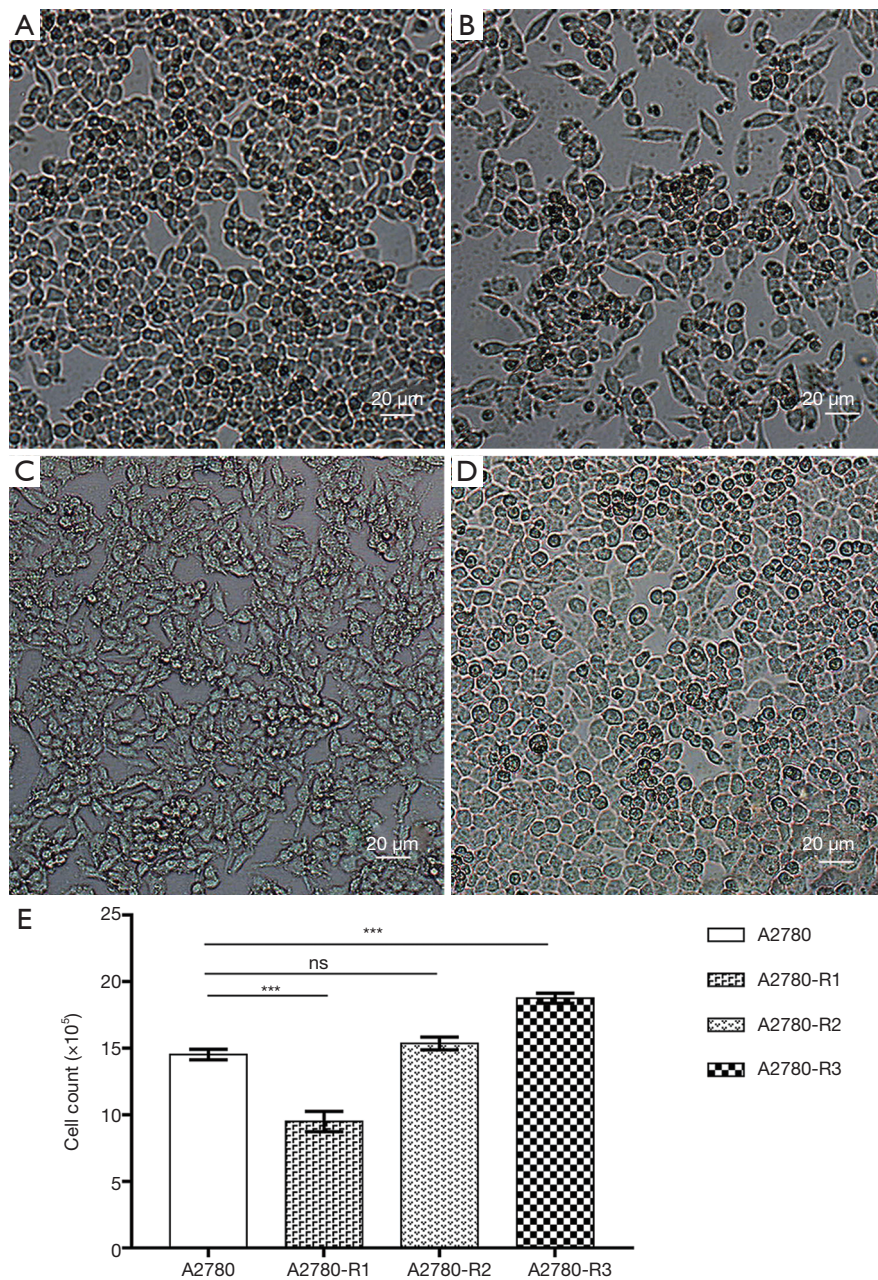
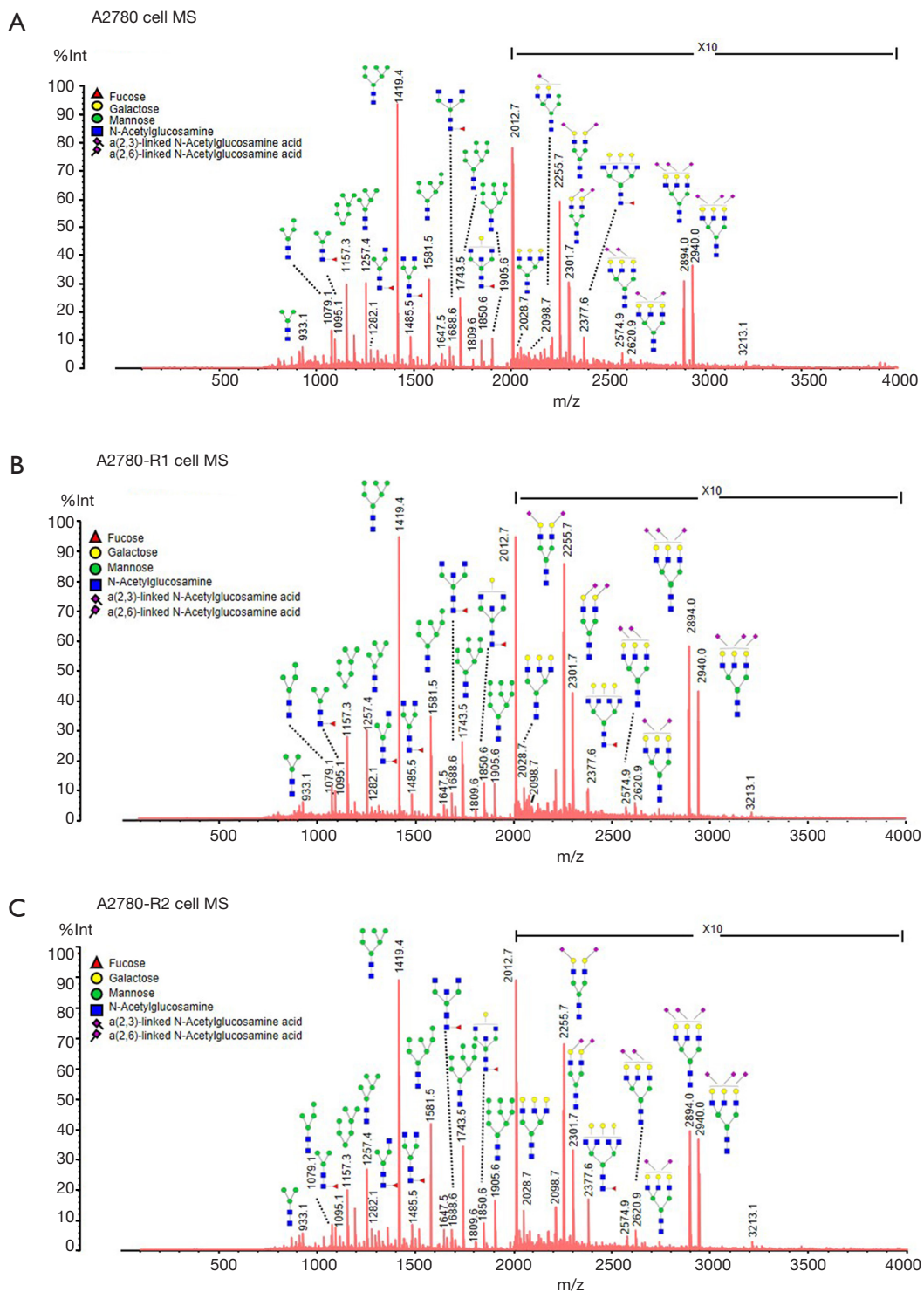


Figure 3 Morphology and growth rate comparison among A2780 cells and three cisplatin-resistant variants. (A,B,C,D) Representative images of A2780 cells and three cisplatin-resistant variants seeded in six-well plates at the same cell density for 48 h; (E) cell counts for A2780 cells and three cisplatin-resistant variants after a 48-h incubation. Error bars: SD (repeated three times); ***, $P < 0.001$, differences were evaluated using Student's *t*-test. SD, standard deviation.

grew slower, A2780-R3 cells were round and grew faster, and A2780-R2 cells had a similar morphology and growth rate (Figure 3E). These data describe the dynamic changes in A2780 cell morphology and growth rates in the process of cisplatin resistance development.

MS analysis of N-glycan profiles in A2780 cells and three cisplatin-resistant variants

To discover the N-glycan alterations among A2780 cells and three cisplatin-resistant variants, a high-sensitivity method was used for the MALDI MS profiling of



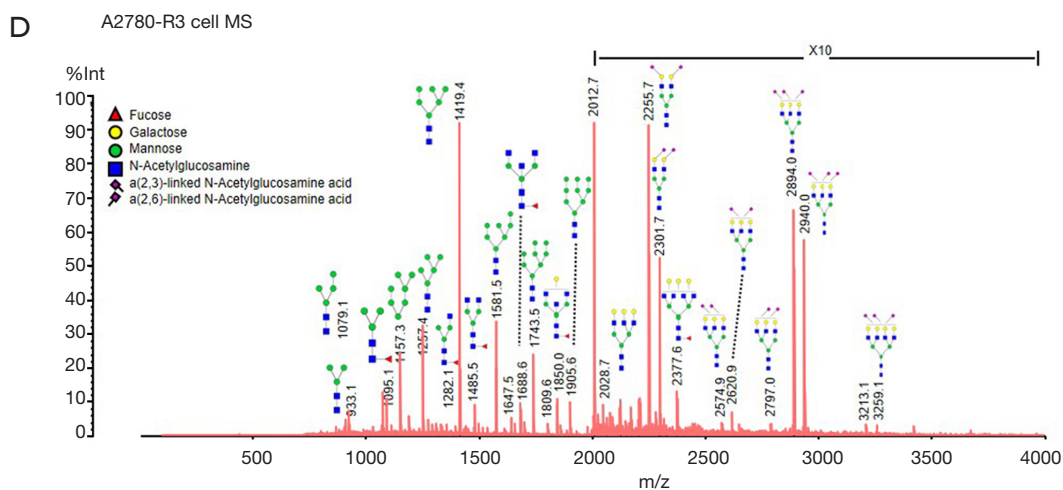


Figure 4 N-glycan quantitative analysis using MALDI-TOF-MS. Representative profile for N-glycans from the whole proteome of A2780 cells and three cisplatin-resistant variants were structurally annotated with putative structures, including mannose, galactose, fucose, N-acetylglucosamine, and sialic acids. (A,B,C,D) MS spectra for A2780 cells and three cisplatin-resistant variants. TOF, time-of-flight; MS, mass spectrometry.

N-glycans (18). A total of 77 N-glycans (peaks) were identified and quantified in all samples (*Figure 4*), including high mannose, hybrid, complex, fucose, bisecting, sialic acid (α 2,3- and α 2,6-linkages), diantennary, tri-antennary, tetra-antennary, and galactose glycoforms. Relative N-glycan intensities in A2780 cells and three cisplatin-resistant variants are shown in *Tables S1,S2,S3*. The up- or down-regulation of the N-glycan levels in three cisplatin-resistant variants was estimated and compared to A2780 cells (*Tables 2,3,4*).

The α 2,3-linked sialic acid was significantly increased in all three cisplatin-resistant variants compared to the parental A2780 cells (*Figure 5A*). Similar increases were also observed in N-glycan gal-ratio (*Figure 5B*). N-glycan gal-ratio was measured from the relative intensities of agalactosylated (signal at m/z 1,485), monogalactosylated (signal at m/z 1,647), and digalactosylated (signal at m/z 1,809) N-glycans according to the formula $G0/(G1+G2 \times 2)$, which was derived from the IgG gal-ratio reported in our previous work (22). Furthermore, high mannose type glycan was slightly increased in three cisplatin-resistant variants (*Figure 5C*). The fucosylated glycans were significantly lower in three cisplatin-resistant variants than in parental A2780 cells (*Figure 5D*). In addition, glyco-subclasses of the α 2,6-linked sialic acid, total sialic acid, hybrid, complex, bisecting GlcNAc, diantennary, tri-antennary, and tetra-

antennary were analyzed. Results did not show significant differences in all three cisplatin-resistant variants compared to the A2780 cells (*Figure 5E,F,G,H,I,J,K,L*). Therefore, the results indicated that the levels of α 2,3-linked sialic acid, N-glycans gal-ratio, high mannose type glycans, and fucosylated glycans are related to the sensitivity of cisplatin in ovarian cancer A2780 cells. Those glyco-subclasses can be used as biomarkers to monitor the development of platinum resistance.

Interestingly, ten glycans displayed significant differences in all three cisplatin-resistant variants compared to A2780 cells, reflecting the dynamic changes in glycans related to cisplatin resistance from A2780 cells to A2780-R3 cells. It was demonstrated that signal at m/z 1,936.6 with α 2,3-linked sialic acid was significantly higher in cisplatin-resistant variants as compared to A2780 cells (*Figure 6A*). Two high-mannose N-glycans (signals at m/z 1,419.4 and 1,581.5) increased and two others (signals at m/z 1,905.6 and 2,067.7) decreased in cisplatin-resistant variants (*Figure 6B,C,D,E*). However, three fucosylated N-glycans (signals at m/z 1,647.5, 1,809.6, and 2,174.8) and two glycans (signals at m/z 1,542.5 and 1,688.6) with bisecting GlcNAc were significantly decreased in cisplatin-resistant variants (*Figure 6F,G,H,I,J*). The dynamic changes of those glycans can be used to monitor the development of platinum resistance in ovarian cancer A2780 cells.

Table 2 List of 34 N-glycans significantly different between A2780 and A2780-R1 cells

m/z	Composition	A2780 (n=3)			A2780-R1 (n=3)			A2780: A2780-R1: B		
		Average	SD	RSD, %	Average	SD	RSD, %	Ratio (B/A)	P value (B/A)	Change (B/A)
1,339.12	H3N4	0.31	0.03	5	0.19	0.08	20	0.61	0.0070	Down
1,419.39	H6N2	8.33	0.31	2	10.30	0.35	2	1.24	0.0001	Up
1,542.52	H3N5	1.14	0.06	3	0.87	0.07	4	0.76	0.0005	Down
1,663.52	H5N4	0.30	0.04	7	0.25	0.03	5	0.83	0.0249	Down
1,688.61	H3N5F1	0.99	0.03	1	0.73	0.10	7	0.74	0.0012	Down
1,704.60	H4N5	0.59	0.07	6	0.43	0.03	4	0.72	0.0022	Down
1,809.58	H5N4F1	3.55	0.20	3	2.81	0.26	5	0.79	0.0015	Down
1,905.64	H9N2	3.71	0.10	1	3.00	0.02	0	0.81	0.0000	Down
1,936.57	H5N4L1	0.08	0.01	7	0.11	0.01	4	1.42	0.0014	Up
1,982.71	H5N4E1	0.22	0.05	11	0.28	0.03	6	1.25	0.0310	Up
2,028.73	H6N5	0.14	0.02	6	0.18	0.03	8	1.25	0.0168	Up
2,067.68	H10N2	0.18	0.03	9	0.14	0.01	2	0.78	0.0123	Down
2,093.74	H4N4L1E1	0.89	0.13	7	1.28	0.08	3	1.44	0.0010	Up
2,128.76	H5N4F1E1	1.40	0.25	9	1.71	0.19	6	1.22	0.0262	Up
2,174.80	H6N5F1	2.40	0.21	4	1.94	0.23	6	0.81	0.0074	Down
2,209.74	H5N4L2	0.77	0.13	8	0.98	0.13	6	1.27	0.0146	Up
2,199.80	H4N6F2	1.11	0.21	10	1.60	0.20	6	1.44	0.0043	Up
2,215.80	H5N6F1	1.94	0.35	9	1.38	0.07	2	0.71	0.0055	Down
2,255.79	H5N4L1E1	1.78	0.09	2	2.99	0.08	1	1.68	0.0000	Up
2,285.80	H5N5F1L1	1.95	0.12	3	1.50	0.13	4	0.77	0.0009	Down
2,301.83	H5N4E2	1.21	0.07	3	1.65	0.09	3	1.36	0.0002	Up
2,377.61	H6N6F1	2.81	0.31	6	1.65	0.05	2	0.59	0.0002	Down
2,447.89	H5N4F1E2	2.02	0.20	5	1.58	0.13	4	0.78	0.0029	Down
2,539.91	H7N6F1	0.71	0.06	4	0.43	0.15	17	0.61	0.0037	Down
2,550.92	H6N6E1	0.80	0.11	7	0.64	0.06	5	0.80	0.0119	Down
2,580.93	H6N7F1	0.40	0.06	7	0.25	0.10	20	0.64	0.0128	Down
2,650.97	H5N5F1E2	1.67	0.23	7	0.92	0.07	4	0.55	0.0004	Down
2,742.98	H7N7F1	0.58	0.18	16	0.24	0.10	21	0.40	0.0044	Down
2,797.03	H6N6L1F2	1.14	0.07	3	2.46	0.41	8	2.16	0.0004	Up
2,813.04	H6N5F1E2	0.78	0.21	13	0.56	0.10	9	0.72	0.0285	Down
2,894.01	H6N5L2E1	1.29	0.07	3	2.74	0.32	6	2.12	0.0001	Up
2,940.05	H6N5L1E2	0.81	0.18	11	1.41	0.25	9	1.75	0.0025	Up
3,016.03	H7N7L1F1	0.51	0.17	17	0.24	0.04	9	0.47	0.0059	Down
3,086.11	H6N5E2L1F1	0.37	0.09	12	0.26	0.05	9	0.70	0.0173	Down

Intensity ratio threshold was set at 1.2 and 0.83 to estimate the up- or down-regulation of the N-glycan levels. RSD, relative standard deviation.

Table 3 List of 6 N-glycans significantly different between A2780 and A2780-R2 cells

m/z	Composition	A2780 (n=3)			A2780-R2 (n=3)			A2780: A2780-R2: C		
		Average	SD	RSD, %	Average	SD	RSD, %	Ratio (C/A)	P value (C/A)	Change (C/A)
933.12	H3N2	0.29	0.01	2	0.28	0.04	8	1.37	0.0000	Up
1,079.14	H3N2F1	0.93	0.18	10	0.92	0.00	0	1.37	0.0027	Up
1,298.13	H4N3	0.31	0.05	8	0.25	0.08	16	0.78	0.0144	Down
1,936.57	H5N4L1	0.08	0.01	7	0.11	0.01	4	1.23	0.0188	Up
2,067.68	H10N2	0.18	0.03	9	0.14	0.01	2	0.81	0.0210	Down
3,132.14	H6N5E3F1	0.12	0.02	9	0.11	0.03	16	1.25	0.0256	Up

Intensity ratio threshold was set at 1.2 and 0.83 to estimate the up- or down-regulation of the N-glycan levels. RSD, relative standard deviation.

Variation of glycome expression in cisplatin-resistant variants of A2780 cells

Transcriptome sequencing and analysis were conducted to identify the differences in glycome expression among A2780 cells and its three cisplatin-resistant variants. Genes involved in N-glycan synthesis that were significantly changed in cisplatin-resistant variants were selected and represented in a heat map (Figure 7A,B,C). In general, transcriptome sequencing results were consistent with the N-glycan alteration analysis. The gene for ST3 beta-galactoside alpha-2,3-sialyltransferase 6 (*ST3GAL6*), which catalyzes the synthesis of the α 2,3-linked sialic acid, has a higher expression in three cisplatin-resistant variants. However, *FUT11* and *FUT1* genes, which encode alpha-(1,3)-fucosyltransferase and galactoside 2-alpha-L-fucosyltransferase 1, respectively, were down-regulated in three cisplatin-resistant variants. Furthermore, GDP-mannose-4,6-dehydratase (*GMDS*) gene, an important player in the fucose biosynthesis pathway, was also decreased in three cisplatin-resistant variants. In addition, expression of the *B4GALT5* gene was decreased in accordance with an increased N-glycan gal-ratio in three cisplatin-resistant variants. Although tri-antennary and tetra-antennary glycans were not significantly elevated in three cisplatin-resistant variants, the *MGAT4A* gene encoding alpha-1,3-mannosylglycoprotein 4-beta-N-acetylglucosaminyltransferase A was slightly increased in all of them. These results were validated via RT-PCR (Figure 7D,E,F,G,H,I). The higher gene expression of *MAN1A1* and *MAN1C1*, encoding class I mammalian Golgi 1,2-mannosidase, which catalyzes the hydrolysis of three terminal mannose residues from peptide-bound Man [9]-GlcNAc [2] oligosaccharides, was identified

in three cisplatin-resistant variants via transcriptome sequencing. However, this result was not in accordance with the RT-PCR analysis as no significant differences in expression were observed between A2780 cells and each cisplatin-resistant variant (data not shown).

Discussion

Ovarian cancer is the second most lethal disease in gynecological malignancies, mainly due to relapse and drug resistance. Most ovarian cancer patients initially respond to platinum compounds and develop platinum resistance following continuous chemotherapy (23). Ovarian cancer patient prognosis after acquiring platinum resistance is extremely poor (10,24). Therefore, it is crucial to conduct studies on the dynamic process during continuous cycles of chemotherapy, which may not only help to develop predictive biomarkers for monitoring platinum resistance, but also provide more information about the mechanisms of platinum resistance and improve patient prognosis. Glycosylation plays an important role in many physiological and pathological processes as well as mechanisms underlying platinum resistance (9,25). There are several glycomic analyses utilized in drug-resistant ovarian cancer. However, none of them concentrate on specific N-glycan changes associated with platinum resistance during continuous cycles of chemotherapy. Furthermore, few glycomic analyses associated with platinum resistance have been performed in cancer cells lines. Cancer cells lines are more readily available and are stable, making them suitable for high-throughput screening. Therefore, this is the first study to identify platinum resistance related to N-glycan changes in ovarian cancer cells during continuous exposure

Table 4 List of 36 N-glycans significantly different between A2780 and A2780-R3 cells

m/z	Composition	A2780 (n=3)			A2780-R3 (n=3)			A2780: A A2780-R3: D		
		Average	SD	RSD, %	Average	SD	RSD, %	Ratio (D/A)	P value (D/A)	Change (D/A)
933.12	H3N2	0.29	0.01	2	0.40	0.03	3	1.39	0.0002	Up
1,079.14	H3N2F1	0.93	0.18	10	1.15	0.19	8	1.24	0.0392	Up
1,095.13	H4N2	0.48	0.10	10	0.66	0.17	13	1.38	0.0308	Up
1,339.12	H3N4	0.31	0.03	5	0.21	0.05	13	0.67	0.0044	Down
1,419.39	H6N2	8.33	0.31	2	10.74	1.40	7	1.29	0.0043	Up
1,542.52	H3N5	1.14	0.06	3	0.82	0.05	3	0.72	0.0002	Down
1,647.54	H4N4F1	5.22	0.42	4	4.30	0.72	8	0.82	0.0188	Down
1,688.61	H3N5F1	0.99	0.03	1	0.79	0.14	9	0.80	0.0089	Down
1,704.60	H4N5	0.59	0.07	6	0.38	0.05	6	0.65	0.0012	Down
1,809.58	H5N4F1	3.55	0.20	3	2.31	0.58	13	0.65	0.0022	Down
1,905.64	H9N2	3.71	0.10	1	2.92	0.12	2	0.79	0.0001	Down
1,936.57	H5N4L1	0.08	0.01	7	0.14	0.05	18	1.83	0.0124	Up
2,067.68	H10N2	0.18	0.03	9	0.14	0.04	13	0.78	0.0472	Down
2,082.72	H5N4F1L1	0.20	0.04	11	0.30	0.04	7	1.46	0.0053	Up
2,093.74	H4N4L1E1	0.89	0.13	7	1.47	0.11	4	1.66	0.0003	Up
2,128.76	H5N4F1E1	1.40	0.25	9	1.81	0.27	8	1.29	0.0185	Up
2,174.80	H6N5F1	2.40	0.21	4	1.95	0.06	2	0.81	0.0021	Down
2,185.78	H5N5E1	1.14	0.15	6	0.90	0.08	4	0.79	0.0072	Down
2,209.74	H5N4L2	0.77	0.13	8	1.01	0.06	3	1.31	0.0041	Up
2,199.80	H4N6F2	1.11	0.21	10	1.56	0.12	4	1.40	0.0032	Up
2,215.80	H5N6F1	1.94	0.35	9	1.30	0.25	10	0.67	0.0066	Down
2,255.79	H5N4L1E1	1.78	0.09	2	3.24	0.27	4	1.81	0.0001	Up
2,285.80	H5N5F1L1	1.95	0.12	3	1.62	0.06	2	0.83	0.0010	Down
2,301.83	H5N4E2	1.21	0.07	3	1.71	0.13	4	1.41	0.0003	Up
2,377.61	H6N6F1	2.81	0.31	6	1.50	0.03	1	0.53	0.0001	Down
2,539.91	H7N6F1	0.71	0.06	4	0.42	0.02	3	0.60	0.0001	Down
2,550.92	H6N6E1	0.80	0.11	7	0.46	0.10	11	0.58	0.0013	Down
2,580.93	H6N7F1	0.40	0.06	7	0.29	0.06	11	0.72	0.0102	Down
2,650.97	H5N5F1E2	1.67	0.23	7	0.79	0.05	3	0.48	0.0002	Down
2,742.98	H7N7F1	0.58	0.18	16	0.29	0.05	9	0.49	0.0056	Down
2,797.03	H6N6L1F2	1.14	0.07	3	2.02	0.21	5	1.78	0.0002	Up
2,813.04	H6N5F1E2	0.78	0.21	13	0.54	0.21	19	0.68	0.0422	Down
2,894.01	H6N5L2E1	1.29	0.07	3	2.52	0.12	2	1.96	0.0000	Up
2,940.05	H6N5L1E2	0.81	0.18	11	1.27	0.10	4	1.57	0.0014	Up
3,016.03	H7N7L1F1	0.51	0.17	17	0.25	0.04	8	0.48	0.0063	Down
3,086.11	H6N5E2L1F1	0.37	0.09	12	0.26	0.08	15	0.70	0.0311	Down

Intensity ratio threshold was set at 1.2 and 0.83 to estimate the up- or down-regulation of the N-glycan levels. RSD, relative standard deviation.

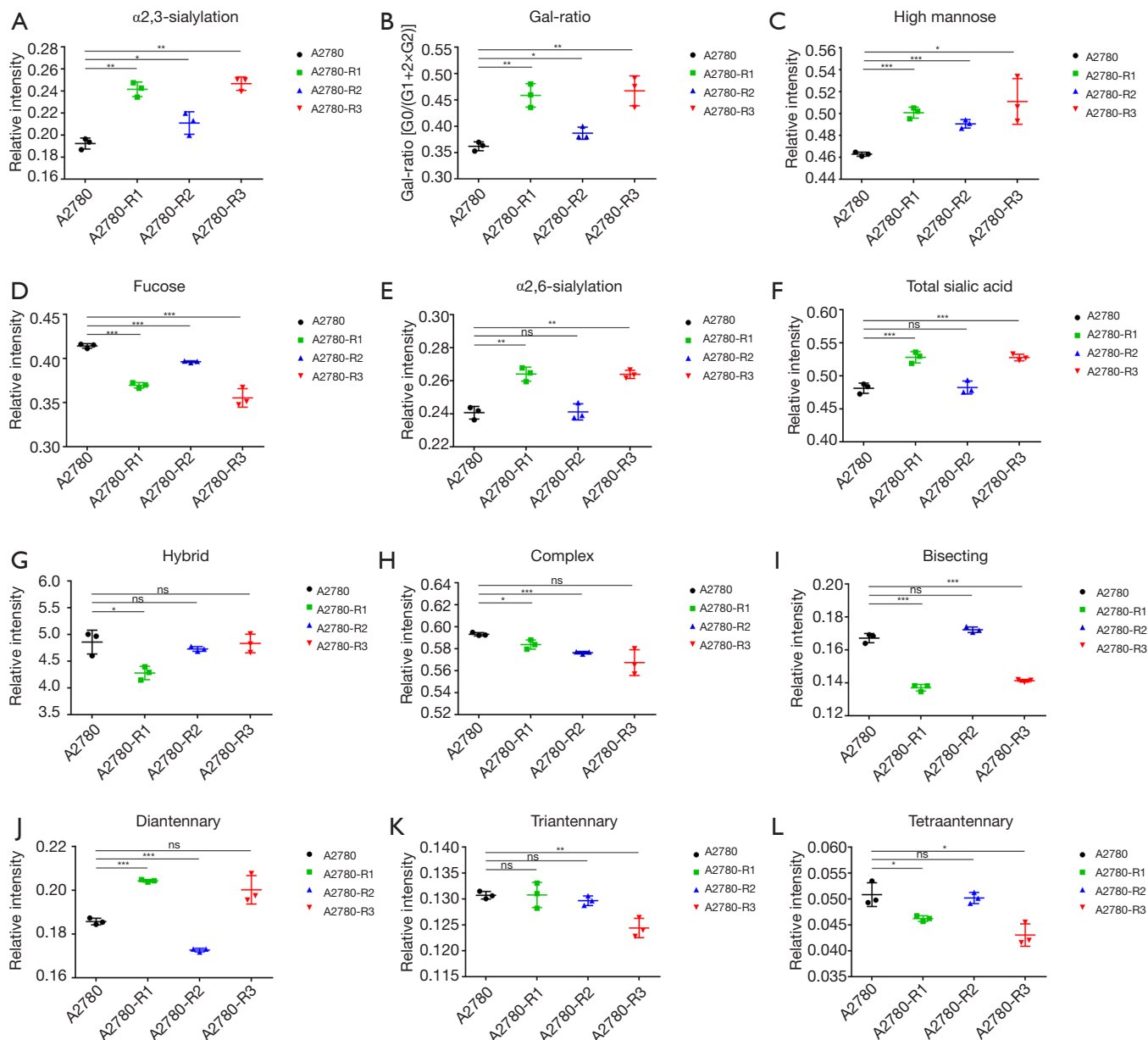


Figure 5 Relative abundance of 12 glyco-subclasses in A2780 cells and three cisplatin-resistant variants. N-glycans were grouped according to their structural features. (A) α 2,3-linked sialic acid; (B) N-glycan gal-ratio [G0/(G1+2xG2)], agalactosylated (G0): 1,485 (H3N4F1), monogalactosyl (G1): 1,647 (H4N4F1), and digalactosyl (G2): 1,809 (H5N4F1); (C) high-mannose; (D) fucose; (E) α 2,6-linked sialic acid; (F) total sialic acid; (G) hybrid; (H) complex; (I) bisecting type; (J,K,L) diantennary, tri-antennary type, and tetra-antennary type glycans. Error bars: SD (repeated three times); *, $P < 0.05$; **, $P < 0.01$; ***, $P < 0.001$, differences were evaluated using Student's *t*-test. SD, standard deviation.

to cisplatin.

The present study mimics the development of platinum resistance in ovarian cancer by continuously exposing A2780 cells to cisplatin. The three cisplatin-resistant variants of the A2780 cells were established after 20, 30,

and 40 continuous exposures to cisplatin, making them relatively stable cisplatin-resistant cells. These cells showed significant differences in improved fold resistance compared to the A2780 cells. More cisplatin-resistant variants could not be selected because of death following

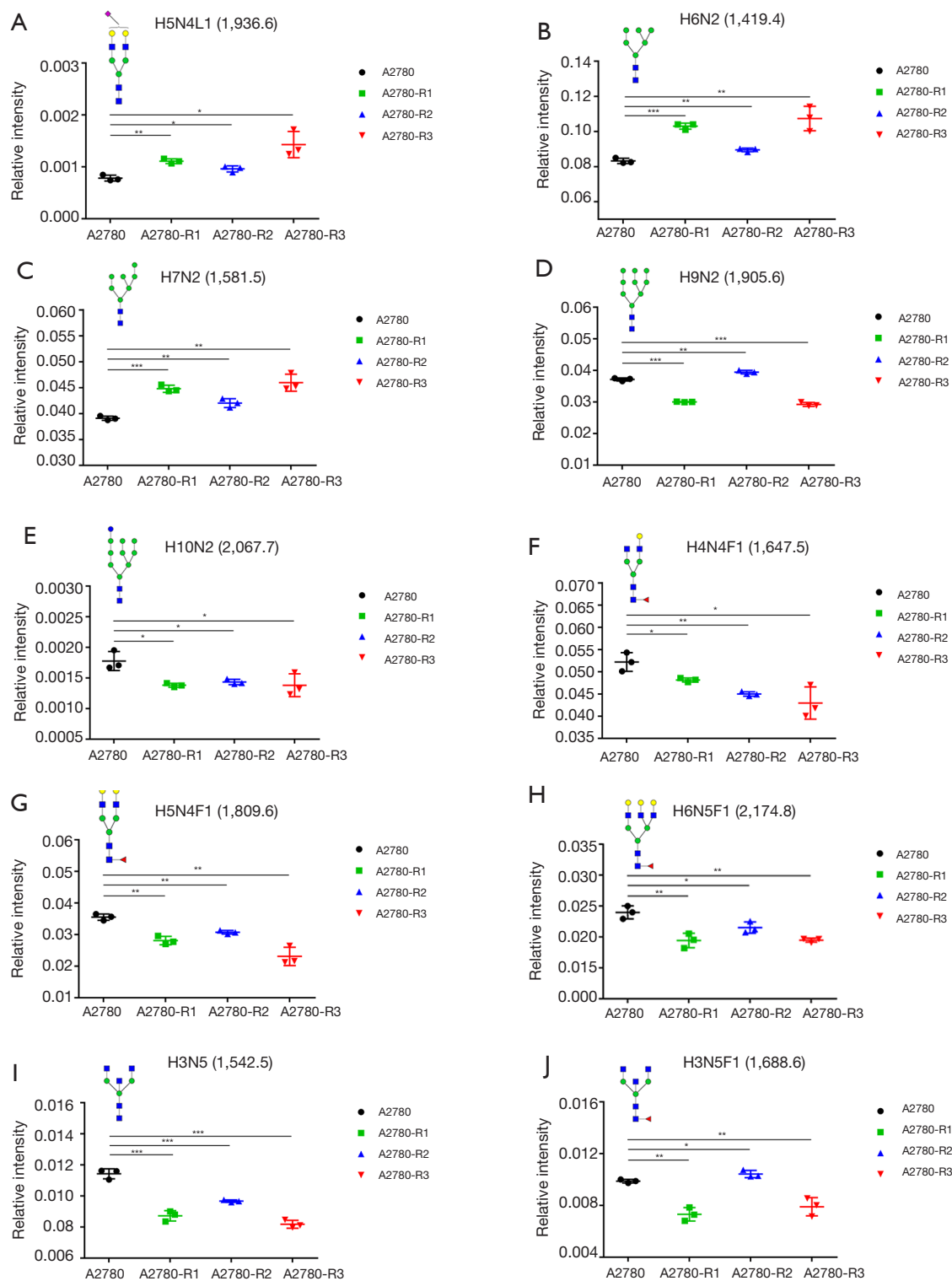


Figure 6 Relative abundance of ten glycans was significantly different in three cisplatin-resistant variants compared to A2780 cells ($P < 0.05$). (A,B,C,D,E,F,G,H,I,J) H5N4L1 (1,936.6); H6N2 (1,419.4); H7N2 (1,581.5); H9N2 (1,905.6); H10N2 (2,067.7); H4N4F1 (1,647.5); H5N4F1 (1,809.6); H6N5F1 (2,174.8); H3N5 (1,542.5); H3N5F1 (1,688.6). Error bars: SD (repeated three times); *, $P < 0.05$; **, $P < 0.01$; ***, $P < 0.001$, differences were evaluated using Student's t -test. SD, standard deviation.

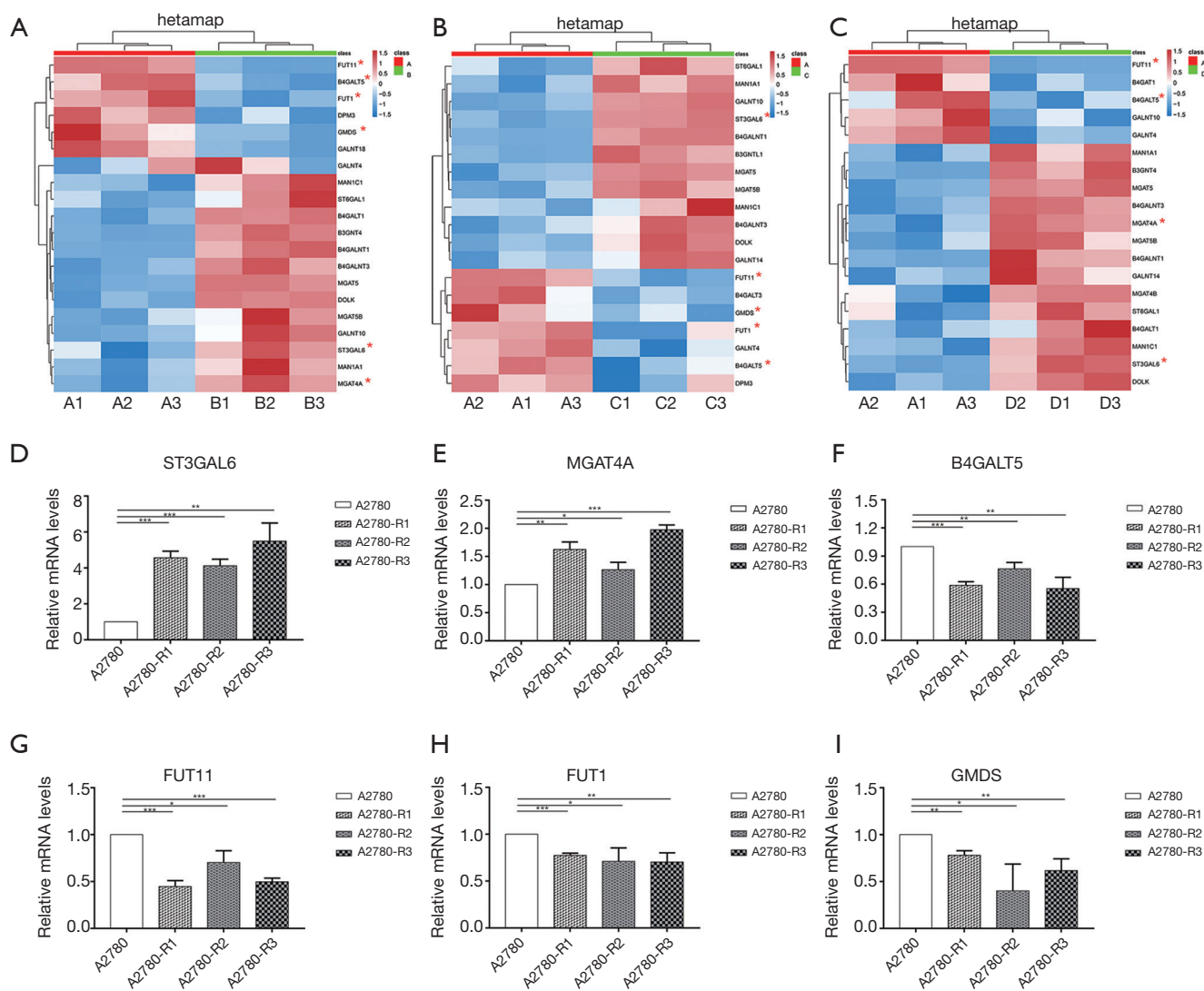


Figure 7 Heat map of altered glycozyme expression in cisplatin-resistant variants compared to A2780 cells. (A) Twenty glycozymes exhibiting significant differences between A2780 and A2780-R1 cells; (B) 19 glycozymes exhibiting significant differences between A2780 and A2780-R2 cells; (C) 19 glycozymes exhibiting significant differences between A2780 and A2780-R3 cells. Genes with * show significant changes, which are consistent well with the RT-PCR validation; (D,E,F,G,H,I) significant changes in genes were validated using RT-PCR (*, $P < 0.05$; **, $P < 0.01$; ***, $P < 0.001$). RT-PCR, real-time PCR.

cisplatin exposure. Then, the higher expression of ABCB1 in cisplatin-resistant variants was identified by RT-PCR and Western-blotting, which indicated the emergence of a resistant phenotype. High-sensitivity MS analysis combined with ethyl esterification derivatization were used to determine N-glycan alterations, including neutral N-glycans and ethyl esterified sialic acid among the four groups, as well as to discriminate between $\alpha 2,3$ - and $\alpha 2,6$ -linkage N-acetylneuraminic acid. Changes in N-glycan

modifications have been mainly attributed to alterations in the corresponding glycosyltransferases (26). Thus, glycozyme expression was analyzed using transcriptome sequencing and further validated via RT-PCR. These results were generally consistent with the MS analysis.

This study demonstrated that expression of $\alpha 2,3$ -linked sialic acid structures and N-glycan gal-ratio increased, while expression of fucosylation structures decreased in three cisplatin-resistant variants compared to A2780 cells. Many

studies have shown that abnormal sialylation is involved in drug resistance. For example, serum levels of α 2,3-sialylated glycans were elevated in drug-resistant oral cancer patients compared to drug-sensitive patients (27). Sialylation was probably involved in the development of multidrug resistance in acute myeloid leukemia cells via *ST3GAL5* or *ST8SIA4* genes (14). Moreover, it has been reported that the *ST6GAL1* gene has a significant impact on multidrug resistance by mediating the PI3K/Akt signaling activity and expression of P-gp and MRP1 (28). *ST6GAL1* sialyltransferase confers cisplatin resistance by reducing the activation of caspase-3 in ovarian cancer cells (29). To the best of our knowledge, this study demonstrated for the first time that both the expression of *ST3GAL6* and α 2,3-sialylated glycans were increased in three cisplatin-resistant variants of ovarian cancer cells, suggesting that α 2,3-sialylation might be involved in cisplatin resistance via *ST3GAL6*.

The IgG gal-ratio was used to evaluate the degree of IgG galactosylation and was found to be significantly higher in 12 types of cancer compared to healthy controls, showing great potential for cancer diagnosis as a pan-cancer biomarker (22). Surprisingly, N-glycan gal-ratio in the current study was increased in three cisplatin-resistant variants of A2780 cells, which might be related to lower expression of *B4GALT5* gene and be a potential biomarker for platinum resistance.

The N-glycomic analyses in this study have shown that high-mannose structures slightly increased and fucosylation structures significantly decreased in three cisplatin-resistant variants of A2780 cells. RT-PCR results also showed that the *FUT11* and *FUT1* genes, which catalyze the transfer of the fucose residue to oligosaccharide acceptor in α 1, 3/4-, and α 1, 2-linkages, were down-regulated in three cisplatin-resistant variants. The lower level of fucosylation structures was further supported by decreased expression of the *GMDS* gene involved in GDP-L-fucose synthesis in cisplatin-resistant variants (30). In line with these results, Zhao *et al.* (25) reported that higher expression of high-mannose structures and lower expression of Fuc α 1-2(gal β 1-4) GlcNAc were identified in the cisplatin-resistant cell line A2780-cp using a lectin blot.

In addition, Alley *et al.* (16) performed the N-linked glycomic analysis of ovarian cancer serum samples and identified that the level of tri- and tetra-antennary structures with varying degrees of sialylation and fucosylation increased accompanied by decreased levels of bisecting oligosaccharides in late-stage recurrent ovarian cancer

patients. However, our MS data suggested that the level of tri- and tetra-antennary were not significantly increased in three cisplatin-resistant variants, although higher gene expression of *MGAT4A* was identified in three cisplatin-resistant variants compared to parental A2780 cells.

Strikingly, compared to A2780 cells, ten N-glycans exhibited significant differences in all three cisplatin-resistant variants, reflecting their dynamic changes from A2780 cells to A2780-R3 cells. These glycans may play a crucial role in cisplatin resistance and can be used as potential biomarkers to monitor the development of cisplatin resistance in ovarian cancer A2780 cells. For example, the higher level of signal at m/z 1936.6 with α 2,3-linked sialic acid and lower level of signal at m/z 1,809.6 with fucosylated glycan might be useful in a clinical setting to monitor the development of platinum resistance.

To the best of our knowledge, this is the first study illustrating N-glycan alterations related to cisplatin resistance in ovarian cancer cells during continuous exposure to cisplatin *in vitro*. These results have an important clinical significance. On one hand, altered N-glycans may serve as biomarkers for monitoring platinum resistance in ovarian cancer patients during continuous cycles of chemotherapy, deserving further study and validation in patient-derived tumor xenografts or clinical samples (31,32). They can be used to monitor patient response to cisplatin treatment during chemotherapy and guide individualized treatment of ovarian cancer patients in a clinical setting. On the other hand, these altered N-glycans might be involved in cisplatin resistance mechanisms. Further study is needed to elucidate this mechanism and provide a better understanding of platinum resistance.

In conclusion, α 2,3-linked sialic structures, found to be increased in cisplatin-resistant variants compared to A2780 cells, might serve as biomarkers to monitor the development of platinum resistance and to guide individualized treatment of ovarian cancer patients.

Acknowledgments

Funding: This work was supported by National Key R&D Program of China (2016YFC1303100) and Natural Science Foundation of China (31770858, 31630088).

Footnote

Conflicts of Interest: The authors have no conflicts of interest to declare.

Ethical Statement: The authors are accountable for all aspects of the work in ensuring that questions related to the accuracy or integrity of any part of the work are appropriately investigated and resolved. Ethics approval was not required as our experiments only use cell lines.

Open Access Statement: This is an Open Access article distributed in accordance with the Creative Commons Attribution-NonCommercial-NoDerivs 4.0 International License (CC BY-NC-ND 4.0), which permits the non-commercial replication and distribution of the article with the strict proviso that no changes or edits are made and the original work is properly cited (including links to both the formal publication through the relevant DOI and the license). See: <https://creativecommons.org/licenses/by-nc-nd/4.0/>.

References

- Lheureux S, Braunstein M, Oza AM. Epithelial ovarian cancer: Evolution of management in the era of precision medicine. *CA Cancer J Clin* 2019;69:280-304.
- Patch AM, Christie EL, Etemadmoghadam D, et al. Whole-genome characterization of chemoresistant ovarian cancer. *Nature* 2015;521:489-94.
- Torre LA, Trabert B, DeSantis CE, et al. Ovarian cancer statistics, 2018. *CA Cancer J Clin* 2018;68:284-96.
- Gonzalez Bosquet J, Newton AM, Chung RK, et al. Prediction of chemo-response in serous ovarian cancer. *Mol Cancer* 2016;15:66.
- Magalhães A, Duarte HO, Reis CA. Aberrant glycosylation in cancer: a novel molecular mechanism controlling metastasis. *Cancer Cell* 2017;31:733-5.
- Agrawal P, Fontanals-Cirera B, Sokolova E, et al. A systems biology approach identifies FUT8 as a driver of melanoma metastasis. *Cancer Cell* 2017;31:804-19.e7.
- Kiermaier E, Moussion C, Veldkamp CT, et al. Polysialylation controls dendritic cell trafficking by regulating chemokine recognition. *Science* 2016;351:186-90.
- Reticker-Flynn NE, Bhatia SN. Aberrant glycosylation promotes lung cancer metastasis through adhesion to galectins in the metastatic niche. *Cancer Discov* 2015;5:168-81.
- Ferreira JA, Peixoto A, Neves M, et al. Mechanisms of cisplatin resistance and targeting of cancer stem cells: Adding glycosylation to the equation. *Drug Resist Updat* 2016;24:34-54.
- Alkema NG, Wisman GB, van der Zee AG, et al. Studying platinum sensitivity and resistance in high-grade serous ovarian cancer: different models for different questions. *Drug Resist Updat* 2016;24:55-69.
- Pinho SS, Seruca R, Gartner F, et al. Modulation of E-cadherin function and dysfunction by N-glycosylation. *Cell Mol Life Sci* 2011;68:1011-20.
- Wojtowicz K, Januchowski R, Nowicki M, et al. Inhibition of protein glycosylation reverses the MDR phenotype of cancer cell lines. *Biomed Pharmacother* 2015;74:49-56.
- Beretta GL, Benedetti V, Cossa G, et al. Increased levels and defective glycosylation of MRPs in ovarian carcinoma cells resistant to oxaliplatin. *Biochem Pharmacol* 2010;79:1108-17.
- Ma H, Zhou H, Song X, et al. Modification of sialylation is associated with multidrug resistance in human acute myeloid leukemia. *Oncogene* 2015;34:726-40.
- Cheng L, Luo S, Jin C, et al. FUT family mediates the multidrug resistance of human hepatocellular carcinoma via the PI3K/Akt signaling pathway. *Cell Death Dis* 2013;4:e923.
- Alley WR, Vasseur JA, Goetz JA, et al. N-linked glycan structures and their expressions change in the blood sera of ovarian cancer patients. *J Proteome Res* 2012;11:2282-300.
- Holst S, Heijs B, de Haan N, et al. Linkage-specific in situ sialic acid derivatization for N-glycan mass spectrometry imaging of formalin-fixed paraffin-embedded tissues. *Anal Chem* 2016;88:5904-13.
- Holst S, Wilding JL, Koprowska K, et al. N-glycomic and transcriptomic changes associated with CDX1 mRNA expression in colorectal cancer cell lines. *Cells* 2019. doi: 10.3390/cells8030273.
- McDermott M, Eustace AJ, Busschots S, et al. In vitro development of chemotherapy and targeted therapy drug-resistant cancer cell lines: a practical guide with case studies. *Front Oncol* 2014;4:40.
- Yan XD, Pan LY, Yuan Y, et al. Identification of platinum-resistance associated proteins through proteomic analysis of human ovarian cancer cells and their platinum-resistant sublines. *J Proteome Res* 2007;6:772-80.
- Vreeker GCM, Nicolardi S, Bladergroen MR, et al. Automated plasma glycomics with linkage-specific sialic acid esterification and ultrahigh resolution MS. *Anal Chem* 2018;90:11955-61.
- Ren S, Zhang Z, Xu C, et al. Distribution of IgG galactosylation as a promising biomarker for cancer screening in multiple cancer types. *Cell Res* 2016;26:963-6.

23. Shin DH, Kwon GS. Pre-clinical evaluation of a chemosensitive gel containing epothilone B and mTOR/Hsp90 targeted agents in an ovarian tumor model. *Journal of Controlled Release* 2017;268:176-83.
24. El Bairi K, Amrani M, Kandhro AH, et al. Prediction of therapy response in ovarian cancer: where are we now? *Crit Rev Clin Lab Sci* 2017;54:233-66.
25. Zhao R, Qin W, Qin R, et al. Lectin array and glycomics expression analyses of ovarian cancer cell line A2780 and its cisplatin-resistant derivative cell line A2780-cp. *Clin Proteomics* 2017;14:20.
26. Kizuka Y, Taniguchi N. Enzymes for N-glycan branching and their genetic and nongenetic regulation in cancer. *Biomolecules* 2016. doi: 10.3390/biom6020025.
27. Shah MH, Telang SD, Shah PM, et al. Tissue and serum alpha 2-3- and alpha 2-6-linkage specific sialylation changes in oral carcinogenesis. *Glycoconj J* 2008;25:279-90.
28. Ma H, Cheng L, Hao K, et al. Reversal effect of ST6GAL1 on multidrug resistance in human leukemia by regulating the PI3K/Akt pathway and the expression of P-gp and MRP1. *PLoS One* 2014;9:e85113.
29. Schultz MJ, Swindall AF, Wright JW, et al. ST6Gal-I sialyltransferase confers cisplatin resistance in ovarian tumor cells. *J Ovarian Res* 2013;6:25.
30. Holst S, Deuss AJ, van Pelt GW, et al. N-glycosylation profiling of colorectal cancer cell lines reveals association of fucosylation with differentiation and caudal type homeobox 1 (CDX1)/villin mRNA expression. *Mol Cell Proteomics* 2016;15:124-40.
31. Cornelison R, Dobbin ZC, Katre AA, et al. Targeting RNA-polymerase I in both chemosensitive and chemoresistant populations in epithelial ovarian cancer. *Clin Cancer Res* 2017;23:6529-40.
32. Boone JD, Dobbin ZC, Straughn JJ, et al. Ovarian and cervical cancer patient derived xenografts: The past, present, and future. *Gynecol Oncol* 2015;138:486-91.

Cite this article as: Lin G, Zhao R, Wang Y, Han J, Gu Y, Pan Y, Ren C, Ren S, Xu C. Dynamic analysis of N-glycomic and transcriptomic changes in the development of ovarian cancer cell line A2780 to its three cisplatin-resistant variants. *Ann Transl Med* 2020;8(6):289. doi: 10.21037/atm.2020.03.12

Table S1 Relative intensities of N-glycans in A2780 cells and its cisplatin-resistant variants

m/z	Composition	A2780 (n=3)		A2780-R1 (n=3)		A2780-R2 (n=3)		A2780-R3 (n=3)		A2780: A A2780-R1: B A2780-R2: C A2780-R3: D					
		Average	RSD, %	Average	RSD, %	Average	RSD, %	Average	RSD, %	Ratio (B/A)	Ratio (C/A)	Ratio (D/A)	P (B/A)	P (C/A)	P (D/A)
933.12	H3N2	0.29	2	0.28	8	0.40	1	0.40	3	0.98	1.37	1.39	0.616	0.000	0.000
1,079.14	H3N2F1	0.93	10	0.92	0	1.27	1	1.15	8	1.00	1.37	1.24	0.944	0.003	0.039
1,095.13	H4N2	0.48	10	0.58	8	0.53	4	0.66	13	1.21	1.12	1.38	0.060	0.150	0.031
1,257.43	H5N2	1.89	8	2.10	5	2.01	5	2.17	7	1.11	1.06	1.15	0.132	0.322	0.095
1,282.14	H3N3F1	0.46	13	0.37	0	0.48	3	0.46	2	0.80	1.04	0.99	0.058	0.622	0.877
1,298.13	H4N3	0.31	8	0.25	16	0.24	6	0.27	7	0.82	0.78	0.87	0.100	0.014	0.092
1,339.12	H3N4	0.31	5	0.19	20	0.32	6	0.21	13	0.61	1.03	0.67	0.007	0.575	0.004
1,403.13	H5N2F1	0.28	4	0.33	8	0.27	6	0.31	9	1.19	0.99	1.13	0.040	0.771	0.121
1,419.39	H6N2	8.33	2	10.30	2	8.95	1	10.74	7	1.24	1.08	1.29	0.000	0.004	0.004
1,444.12	H4N3F1	0.45	4	0.41	3	0.46	4	0.50	5	0.92	1.02	1.11	0.036	0.552	0.060
1,460.01	H5N3	0.20	6	0.20	5	0.17	1	0.18	12	1.00	0.84	0.90	0.919	0.009	0.241
1,485.52	H3N4F1	4.46	3	4.78	3	4.19	3	4.15	4	1.07	0.94	0.93	0.035	0.053	0.068
1,501.53	H4N4	0.24	5	0.20	15	0.24	7	0.23	7	0.81	1.00	0.96	0.067	0.979	0.418
1,542.52	H3N5	1.14	3	0.87	4	0.97	1	0.82	3	0.76	0.85	0.72	0.001	0.001	0.000
1,581.52	H7N2	3.91	1	4.48	2	4.20	2	4.60	4	1.15	1.07	1.18	0.000	0.006	0.002
1,622.51	H5N3F1	0.21	1	0.21	14	0.20	22	0.21	13	1.00	0.96	1.01	0.955	0.767	0.872
1,647.54	H4N4F1	5.22	4	4.82	1	4.50	1	4.30	8	0.92	0.86	0.82	0.032	0.005	0.019
1,663.52	H5N4	0.30	7	0.25	5	0.33	9	0.27	6	0.83	1.09	0.90	0.025	0.273	0.144
1,688.61	H3N5F1	0.99	1	0.73	7	1.04	3	0.79	9	0.74	1.06	0.80	0.001	0.037	0.009
1,704.60	H4N5	0.59	6	0.43	4	0.58	6	0.38	6	0.72	0.99	0.65	0.002	0.785	0.001
1,743.49	H8N2	5.13	1	5.01	2	5.27	2	4.99	3	0.98	1.03	0.97	0.141	0.090	0.271
1,809.58	H5N4F1	3.55	3	2.81	5	3.07	2	2.31	13	0.79	0.87	0.65	0.002	0.002	0.002
1,820.62	H4N4E1	0.15	4	0.15	5	0.11	9	0.12	23	1.04	0.73	0.83	0.004	0.157	0.828
1,850.59	H4N5F1	1.08	2	0.91	8	1.20	2	1.05	2	0.84	1.12	0.98	0.016	0.002	0.167
1,866.58	H5N5	0.27	6	0.23	4	0.25	6	0.23	20	0.85	0.92	0.85	0.022	0.172	0.235
1,891.61	H3N6F1	0.17	3	0.17	3	0.17	4	0.18	8	0.96	1.00	1.07	0.117	0.952	0.287
1,905.64	H9N2	3.71	1	3.00	0	3.95	1	2.92	2	0.81	1.06	0.79	0.000	0.005	0.000
1,936.57	H5N4L1	0.08	7	0.11	4	0.10	6	0.14	18	1.42	1.23	1.83	0.001	0.019	0.012
1,966.71	H4N4F1E1	0.18	13	0.17	7	0.16	10	0.15	19	0.92	0.87	0.81	0.396	0.239	0.176
1,982.71	H5N4E1	0.22	11	0.28	6	0.19	6	0.28	14	1.25	0.86	1.26	0.031	0.108	0.091
2,012.73	H5N5F1	1.60	3	1.40	2	1.82	2	1.54	6	0.88	1.14	0.97	0.004	0.003	0.419
2,028.73	H6N5	0.14	6	0.18	8	0.13	6	0.15	5	1.25	0.95	1.09	0.017	0.352	0.136
2,053.82	H4N6F1	0.09	16	0.10	16	0.08	12	0.10	10	1.03	0.83	1.07	0.811	0.187	0.552
2,067.68	H10N2	0.18	9	0.14	2	0.14	3	0.14	13	0.78	0.81	0.78	0.012	0.021	0.047
2,082.72	H5N4F1L1	0.20	11	0.23	13	0.23	5	0.30	7	1.13	1.12	1.46	0.283	0.083	0.005
2,093.74	H4N4L1E1	0.89	7	1.28	3	1.19	5	1.47	4	1.44	0.99	1.66	0.001	0.084	0.000
2,098.72	H6N4L1	0.80	6	0.70	7	0.81	4	0.80	6	0.87	1.02	1.00	0.053	0.708	0.964
2,128.76	H5N4F1E1	1.40	9	1.71	6	1.43	11	1.81	8	1.22	1.02	1.29	0.026	0.829	0.018
2,140.75	H5N5L1	1.28	6	1.26	10	1.28	2	1.39	5	0.98	1.00	1.08	0.805	0.986	0.148
2,158.78	H5N5F2	1.12	8	1.26	3	1.30	7	1.26	3	1.12	1.16	1.12	0.061	0.069	0.066
2,174.80	H6N5F1	2.40	4	1.94	6	2.15	4	1.95	2	0.81	0.90	0.81	0.007	0.037	0.002
2,185.78	H5N5E1	1.14	6	0.99	11	1.20	7	0.90	4	0.87	1.05	0.79	0.107	0.374	0.007
2,209.74	H5N4L2	0.77	8	0.98	6	0.93	3	1.01	3	1.27	0.95	1.31	0.015	0.374	0.004
2,199.80	H4N6F2	1.11	10	1.60	6	1.06	3	1.56	4	1.44	0.96	1.40	0.004	0.513	0.003
2,215.80	H5N6F1	1.94	9	1.38	2	1.89	3	1.30	10	0.71	0.97	0.67	0.005	0.668	0.007
2,255.79	H5N4L1E1	1.78	2	2.99	1	1.64	7	3.24	4	1.68	0.92	1.81	0.000	0.107	0.000
2,285.80	H5N5F1L1	1.95	3	1.50	4	2.04	5	1.62	2	0.77	1.04	0.83	0.001	0.244	0.001
2,301.83	H5N4E2	1.21	3	1.65	3	1.26	5	1.71	4	1.36	1.04	1.41	0.000	0.337	0.000
2,331.85	H5N5F1E1	0.68	1	0.66	14	0.72	13	0.79	8	0.97	1.06	1.16	0.682	0.493	0.034
2,347.85	H6N5E1	1.03	6	0.92	4	0.97	6	0.90	3	0.89	0.94	0.88	0.055	0.289	0.029
2,355.81	H5N4F1L2	0.71	21	0.78	6	0.74	17	0.82	12	1.09	1.04	1.16	0.510	0.810	0.334
2,377.61	H6N6F1	2.81	6	1.65	2	2.58	2	1.50	1	0.59	0.92	0.53	0.000	0.066	0.000
2,393.74	H7N6	0.43	6	0.47	1	0.50	9	0.46	15	1.09	1.18	1.08	0.064	0.061	0.476
2,412.83	H5N5L2	0.62	21	0.61	7	0.59	6	0.63	3	0.99	0.96	1.03	0.933	0.770	0.835
2,447.89	H5N4F1E2	2.02	5	1.58	4	1.95	7	1.70	7	0.78	0.97	0.84	0.003	0.536	0.024
2,459.67	H5N5L1E1	0.54	12	0.60	12	0.55	12	0.55	17	1.11	1.02	1.02	0.356	0.841	0.896
2,539.91	H7N6F1	0.71	4	0.43	17	0.69	6	0.42	3	0.61	0.97	0.60	0.004	0.486	0.000
2,550.92	H6N6E1	0.80	7	0.64	5	0.79	6	0.46	11	0.80	0.99	0.58	0.012	0.806	0.001
2,574.89	H6N5L2	0.40	22	0.59	18	0.52	5	0.54	15	1.46	1.29	1.34	0.080	0.098	0.125
2,580.93	H6N7F1	0.40	7	0.25	20	0.48	7	0.29	11	0.64	1.19	0.72	0.013	0.052	0.010
2,620.93	H6N5L1E1	0.72	10	0.75	5	0.71	5	0.67	9	1.05	1.00	0.94	0.485	0.975	0.444
2,650.97	H5N5F1E2	1.67	7	0.92	4	1.66	4	0.79	3	0.55	0.99	0.48	0.000	0.891	0.000
2,666.96	H6N5E2	0.43	15	0.38	6	0.50	8	0.35	7	0.89	1.18	0.83	0.295	0.165	0.146
2,720.94	H6N5F1L2	0.62	9	0.51	13	0.67	6	0.57	10	0.83	1.09	0.92	0.099	0.234	0.307
2,742.98	H7N7F1	0.58	16	0.24	21	0.51	7	0.29	9	0.40	0.88	0.49	0.004	0.279	0.006
2,766.98	H6N5F1L1E1	0.51	11	0.54	18	0.53	11	0.51	5	1.04	1.02	0.98	0.748	0.807	0.801
2,797.03	H6N6L1F2	1.14	3	2.46	8	1.10	3	2.02	5	2.16	0.97	1.78	0.000	0.299	0.000
2,813.04	H6N5F1E2	0.78	13	0.56	9	0.72	3	0.54	19	0.72	0.91	0.68	0.028	0.333	0.042
2,894.01	H6N5L2E1	1.29	3	2.74	6	1.48	17	2.52	2	2.12	1.15	1.96	0.000	0.250	0.000
2,940.05	H6N5L1E2	0.81	11	1.41	9	0.83	14	1.27	4	1.75	1.03	1.57	0.002	0.807	0.001
2,986.09	H6N5E3	0.21	19	0.17	13	0.17	11	0.16	13	0.81	0.84	0.80	0.202	0.256	0.179
2,994.03	H6N5L3F1	0.17	20	0.14	15	0.18	9	0.14	15	0.83	1.09	0.85	0.266	0.526	0.324
3,016.03	H7N7L1F1	0.51	17	0.24	9	0.45	6	0.25	8	0.47	0.89	0.48	0.006	0.328	0.006
3,040.07	H6N5F1L2E1	0.14	7	0.14	4	0.16	6	0.14	9	0.98	1.17	1.02	0.662	0.041	0.759
3,086.11	H6N5E2L1F1	0.37	12	0.26	9	0.35	17	0.26	15	0.70	0.95	0.70	0.017	0.677	0.031
3,132.14	H6N5E3F1	0.12	9	0.11	16	0.16	7	0.14	13	0.85	1.25	1.16	0.188	0.026	0.197
3,213.10	H7N6L3	0.13	7	0.11	10	0.15	19	0.13	9	0.84	1.14	0.94	0.061	0.342	0.404

The RSD was below 25%. H, hexose; N, N-acetylhexosamine; F, deoxyhexose (fucose); L, lactonized N-acetylneuraminic acid (α 2,3-linked); E, ethyl. RSD, relative standard deviation.

Table S2 Relative intensities of glyco-subclasses in A2780 cells and its cisplatin-resistant variants

Derived traits	A2780	A2780-R1	A2780-R2	A2780-R3	A2780: A A2780-R1: B A2780-R2: C A2780-R3: D					
	Average	Average	Average	Average	Ratio (B/A)	Ratio (C/A)	Ratio (D/A)	P (B/A)	P (C/A)	P (D/A)
High-Mannose type in total spectrum	23.42	25.37	24.80	25.68	1.08	1.06	1.10	0.000	0.000	0.016
Hybrid type in total spectrum	2.43	2.14	2.36	2.42	0.88	0.97	0.99	0.017	0.380	0.882
Complex type in total spectrum	59.31	36.95	39.64	35.53	0.98	0.97	0.96	0.022	0.000	0.193
Fucosylated species of complex glycans in spectrum	41.42	13.70	17.22	14.12	0.89	0.96	0.86	0.000	0.000	0.001
Bisected species of complex glycans in spectrum	16.71	20.43	17.26	20.02	0.82	1.03	0.85	0.000	0.055	0.000
Diantennary species of complex glycans in spectrum	18.57	13.08	12.97	12.44	1.10	0.93	1.08	0.000	0.000	0.197
Triantennary species of complex glycans in spectrum	13.07	13.08	12.97	12.44	1.00	0.99	0.95	0.974	0.197	0.005
Tetraantennary species of complex glycans in spectrum	5.08	4.62	5.02	4.30	0.91	0.99	0.85	0.027	0.677	0.013
Sialylated species of complex glycans in spectrum	43.28	50.55	45.20	51.04	1.17	1.04	1.18	0.001	0.084	0.000
α 2,3-sialylation of complex glycans in spectrum	19.22	24.15	21.08	24.66	1.26	1.10	1.28	0.000	0.047	0.000
α 2,6-sialylation of complex glycans in spectrum	24.06	26.40	24.11	26.38	1.10	1.00	1.10	0.002	0.887	0.001
Gal-ratio [G0/(G1+2xG2)]	0.18	0.23	0.19	0.23	1.27	1.09	1.29	0.002	0.026	0.004

Attention: G0:1,485 (H3N4F1); G1:1,647 (H4N4F1); G2:1,809 (H5N4F1).

Table S3 Calculations MALDI-TOF-MS

- (I) High-Mannose type in total spectrum: 1,257.43+1,403.13+1,419.39+1,581.52+1,743.49+1,905.64+2,067.68
- (II) Hybrid type in total spectrum: 1,282.14+1,298.13+1,444.12+1,460.01+1,622.51+2,098.72
- (III) Complex type in total spectrum: 933.12+1,079.14+1,095.13+1,339.12+1,485.52+1,501.53+1,542.52+1,647.54+1,663.52+1,688.61+1,704.60+1,809.58+1,820.62+1,850.59+1,866.58+1,891.61+1,936.57+1,966.71+1,982.71+2,012.73+2,028.73+2,053.82+2,082.76+2,093.74+2,128.76+2,140.75+2,158.78+2,174.80+2,185.78+2,209.74+2,199.74+2,215.80+2,255.79+2,285.80+2,301.83+2,331.85+2,347.85+2,355.81+2,377.61+2,393.74+2,412.83+2,447.89+2,459.67+2,539.91+2,550.92+2,574.89+2,580.93+2,620.93+2,650.97+2,666.96+2,720.94+2,742.98+2,766.98+2,797.03+2,813.04+2,894.01+2,940.05+2,986.09+2,994.03+3,016.03+3,040.07+3,086.11+3,132.14+3,213.10
- (IV) Fucosylated species of complex glycans in spectrum: 1,485.52+1,647.54+1,688.61+1,809.58+1,850.59+1,891.61+1,966.71+2,012.73+2,053.82+2,082.76+2,128.76+2,158.78+2,174.80+2,199.74+2,215.80+2,285.80+2,331.85+2,355.81+2,377.61+2,447.89+2,539.91+2,580.93+2,650.97+2,720.94+2,742.98+2,766.98+2,797.03+2,813.04+2,994.03+3,016.03+3,040.07+3,086.11+3,132.14
- (V) Bisected species of complex glycans in spectrum: 1,542.52+1,688.61+1,704.60+1,850.59+1,866.58+2,012.73+2,140.75+2,158.78+2,285.80+2,331.85+2,412.83+2,459.67+2,580.93+2,650.97+2,742.98+3,016.03
- (VI) Diantennary species of complex glycans in spectrum: 1,339.12+1,485.52+1,501.53+1,647.54+1,663.52+1,850.59+1,866.58+1,936.57+1,966.71+1,982.71+2,082.76+2,128.76+2,209.74+2,255.79+2,301.83+2,355.81
- (VII) Triantennary species of complex glycans in spectrum: 2,082.76+2,174.80+2,347.85+2,377.61+2,574.89+2,620.93+2,666.96+2,720.94+2,766.98+2,813.04+2,894.01+2,940.05+2,986.09+2,994.03+3,040.07+3,086.11+3,132.14+3,213.10
- (VIII) Tetraantennary species of complex glycans in spectrum: 2,053.82+2,199.74+2,215+2,393.74+2,539.91+2,550.92
- (IX) Sialylated species of complex glycans in spectrum: α 2,3-sialylation of complex glycans + α 2,6-sialylation of complex glycans
- (X) α 2,3-sialylation of complex glycans in spectrum: (2,093.74+2,209.74+2,355.81+2,412.83+2,994.03) + 1/2(1,936.57+2,082.76+2,140.75+2,255.79+2,285.80+2,459.67) + 2/3(2,574.89+2,720.94+2,894.01+3,040.07) + 1/3(2,620.93+2,766.98+2,797.03+2,940.05+3,086.11) + 3/4(3,213.10) + 1/4(3,016.03)
- (XI) α 2,6-sialylation of complex glycans in spectrum: (1,820.62+1,966.71+2,093.74+2,301.83+2,447.89+2,650.97+2,986.09+3,132.14) + 1/2(2,128.76+2,185.78+2,255.79+2,331.85+2,459.67) + 1/3(2,347.85+2,620.93+2,766.98+2,894.01+3,040.07) + 2/3(2,666.96+2,813.04+2,940.05+3,086.11)
- (XII) Gal-ratio [G0/(G1+2xG2)]:{1,485.52/[1,647.54+2(1,809.58)]}

TOF, time-of-flight; MS, mass spectrometry.